

EPR and evidence for two structural
nonequivalent states of Tl^{2+} (II) paramagnetic
centers near noncentral positions in Rb_2SO_4 and
 Cs_2SO_4 crystals

G.V. Mamin and V.N. Efimov

Kazan State University, Kremlevskaya, 18, Kazan 420008, Russia

E-mail: george.mamin@ksu.ru, vladimir.efimov@ksu.ru

Received September 10, 1999

Accepted October 5, 1999



Volume 3
No. 2, 1997

Abstract

The EPR spectrum temperature dependence of $Tl^{2+}(\text{II})$ paramagnetic centers in Rb_2SO_4 , Cs_2SO_4 crystals have been investigated. At $100K > T > 40K$ the local symmetry of $Tl^{2+}(\text{II})$ paramagnetic centers is C_1 . The broadening and doubling of EPR spectrum lines with decreasing of $T < 40K$ were observed. The angular dependence of lines positions indicate that two structural nonequivalent positions of $Tl^{2+}(\text{II})$ paramagnetic center exist at $T < 20K$. The measurement of dielectric constant of crystals displayed the absence of phase transition in this temperature range. The transformation of EPR spectrum is explained by motion of $Tl^{2+}(\text{II})$ paramagnetic center between two structural nonequivalent states arising near noncentral positions. Parameters of the potential have been extracted by fitting of the temperature dependence of EPR spectrum. Two nonequivalent states are possible due to large difference between ionic radius of Tl^{2+} and Rb^+ , Cs^+ .

PACS : 71.55; 76.30

Keywords : Electron paramagnetic resonance, noncentral ions, local dynamics

The EPR method detects the noncentrality of the impurity paramagnetic $Tl^{2+}(\text{II})$ ions in K_2SO_4 , Rb_2SO_4 and Cs_2SO_4 crystals [1]. These defects perform the activation motion within the two potential wells along the c axis of the crystal. The activation motion parameters ($E_a=0.06$ eV, $\tau_0=5\cdot 10^{-13}$ s) corresponds to noncentral jumps [1, 2]. This defects motion leads to broadening and doubling of EPR spectrum lines. The temperatures of the broadening are different for each crystals ($T_{K_2SO_4}=30-50$ K, $T_{Rb_2SO_4}=80-110$ K, $T_{Cs_2SO_4}=70-100$ K).

However, at low temperature ($T\sim 15-60$ K) in Rb_2SO_4 and Cs_2SO_4 crystals the additional doubling of EPR lines was observed [1]. This splitting testify the appearance of two structural non-equivalent $Tl^{2+}(\text{II})$ centers (Fig. 2, 4). Since the phase transitions exists in some crystals of K_2SO_4 group, we suppose that the additional anomaly of EPR spectra can be associated with the structural phase transition. This suggestion have been confirmed by the anomaly in temperature dependence of B_2^0 spin-hamiltonian parameter of Mn^{2+} ions in Cs_2SO_4 [3]. In the present paper we report additional studies of low temperature anomalies of $Tl^{2+}(\text{II})$ EPR spectra in Rb_2SO_4 and Cs_2SO_4 crystals.

To determine the nature of anomalies we have measured the temperature dependence of dielectric constant ε in Rb_2SO_4 and Cs_2SO_4 crystals with 0.1-0.5% thallium impurity in the temperature range which corresponds to the transformation of EPR spectra (Fig. 1). However, no anomalies of the temperature dependence of ε have been detected. This confirms the absence of ferroelectric phase transitions in Cs_2SO_4 crystals.

The temperature dependence of $Tl^{2+}(\text{II})$ ions EPR spectrum in Cs_2SO_4 crystals is shown in Fig. 2a. The similar transformation of line shape is appeared when the EPR spectrum averaged by the motion of defects between two states with not equal occupation probabilities [4]. This transformation can be described by Bloch equations, which were modified for defects motion processes [4]. The magnetic moment, whose imaginary part is proportional to EPR absorption, can be written as

$$\widehat{M} = K \frac{f_a (H - \widehat{H}_b) + f_b (H - \widehat{H}_a)}{\left[(H - \widehat{H}_a) + iAP_{ab} \right] \left[(H - \widehat{H}_b) + iAP_{ba} \right] + A^2 P_{ab} P_{ba}}, \quad (1)$$

where P_{ab} - the probability of defect jump from a state to b state, P_{ba} - the jump probability from b state to a state, $f_a = \frac{P_{ba}}{P_{ab}+P_{ba}}$ and $f_b = \frac{P_{ab}}{P_{ab}+P_{ba}}$ are the populations of potential minima, $\widehat{H}_{a,b} = H_{a,b} + i\frac{1}{AT_2}$, H_a, H_b - magnetic field corresponding to the EPR of defect in a or b state, T_2 - spin-spin relaxation time, $A = \frac{4\pi\nu_{EPR}}{H_a+H_b}$. The intensities of line for defects in a and b states are different at low temperatures indicating minima of multi-well potential with various depths. The probabilities P_{ab} and P_{ba} can be written from Arrhenius activation law

$$P_{ab} = \frac{1}{\tau_0} \exp\left(-\frac{E_a}{kT}\right), P_{ba} = \frac{1}{\tau_0} \exp\left(-\frac{E_a - E_0}{kT}\right), \quad (2)$$

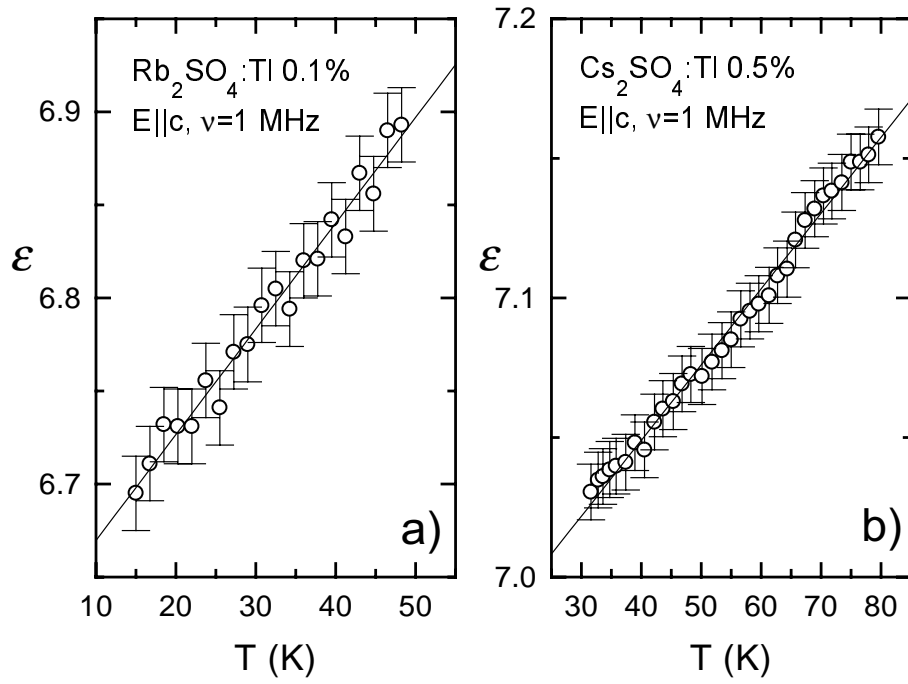


Figure 1: The temperature dependence of dielectric constant in a) Rb_2SO_4 and b) Cs_2SO_4 crystals

where E_a - the activation energy, E_0 - the difference between depths of potential minima. We substituted 2 in the equation 1 and calculated EPR line shape. The result of fitting is shown on Fig. 2a by dotted line. One can see that experimental EPR spectra can be approximated by the model of Tl^{2+} (II) ions motion in non symmetric two well potential with parameters shown in table 1.

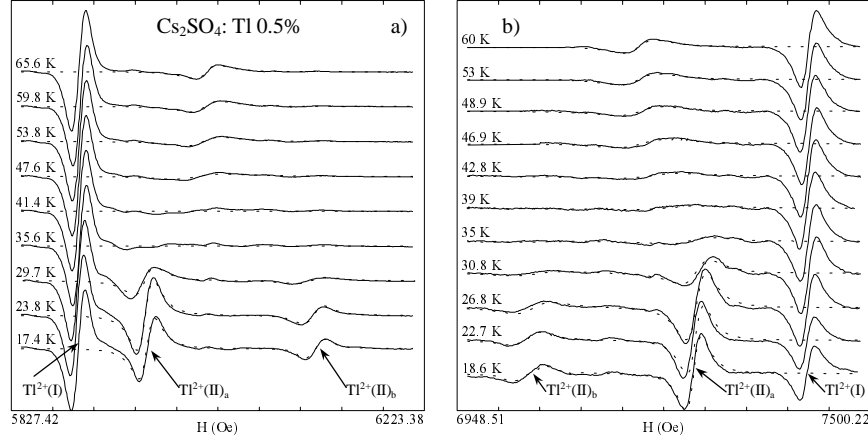


Figure 2: The temperature dependence of EPR spectra transformation in case of a) low-field and b) high-field transitions at $\mathbf{H}||\mathbf{a}$. The solid line - experimental data, dotted line - approximation by equation 1.

Table 1. Parameters of thallium motion in two-well energy potential.

Crystals	E_a (eV)	E_0 (eV)	τ_0 (10^{-11} s)
Rb ₂ SO ₄	0.026±0.001	0.004±0.0001	1±0.3
Cs ₂ SO ₄	0.019±0.001	0.002±0.0001	1.1±0.3

If this transformation corresponds to the defect motion, but not phase transition, the splitting temperature T^* must depend on $\Delta H = H_a - H_b$. The ΔH value was measured at low temperature, when jumps between states of defects are frozen. The Tl^{2+} ions have $[Xe]f^{14}5d^{10}6s^1$ electron shell configuration. Because of the strong contact interaction of 6s electron with ion's nucleus, the hyperfine structure constant is big ($A_{hfs} \approx 110$ GHz $\gg g\beta H$). The big A_{hfs} value leads to two EPR hyperfine transitions with different ΔH values. The temperature dependencies of EPR line form for two hyperfine transitions with $\Delta H = 162$ Oe and $\Delta H = 221$ Oe are shown in Fig. 2 a, b. However, as one can see, the temperature range of spectrum transformation is wider, than possible shift of T^* . The E_a , E_0 and τ_0 parameters were obtained from approximation of the line shape transformation of high-field hyperfine EPR transition by equations 1, 2. The values of this parameters are nearly equal to those obtained for the low-field hyperfine transition (Fig. 2 a). This indicates, that Tl^{2+} (II) ions

in Rb_2SO_4 , Cs_2SO_4 crystals are involved in additional motion. This type of motion is absent in K_2SO_4 crystals but appears in Rb_2SO_4 , Cs_2SO_4 crystals, when the radius of thallium ions is less than the radius of the substituted cation ($R_{\text{Tl}^{2+}}=1.36 \text{ \AA}$, $R_{\text{K}^+}=1.33 \text{ \AA}$, $R_{\text{Rb}^+}=1.49 \text{ \AA}$, $R_{\text{Cs}^+}=1.65 \text{ \AA}$ [5]). Therefore we can assume, that this motion can appear due to of Coulomb interaction of thallium ion with surrounding ions. The calculated potential of $\text{Tl}^{2+}(\text{II})$ ions for K_2SO_4 , Rb_2SO_4 , Cs_2SO_4 crystals is shown in Fig. 3

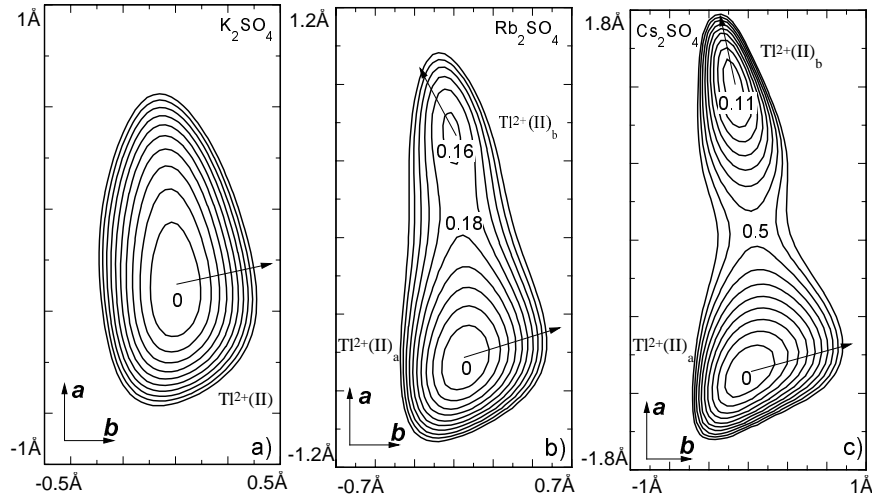


Figure 3: The energy potential of $\text{Tl}^{2+}(\text{II})$ ions in the cation position of a) K_2SO_4 , b) Rb_2SO_4 , c) Cs_2SO_4 crystals. The energy unit is eV. The arrows show the direction of z axis projection of \hat{g}^{2*} -tensor on (ab) plane of crystal.

In our calculations we used the following assumptions:

1. The calculation of the electrostatic field was implemented in point charge model.
2. The ion's position was fixed.
3. The electron shell of oxygen ions was assumed to be a sphere.
4. The energy repulsion between oxygen and thallium ions was taken as

$$E = E_o \exp\left(-\frac{R_{\text{Tl}-\text{O}}}{\rho_o}\right), \quad (3)$$

where $E_o = E_{\text{Cl}} = 1.2 \cdot 10^4 \text{ eV}$, $\rho_o = \rho_{\text{Cl}} - R_{\text{Cl}} + R_o = 0.23 \text{ \AA}$. The E_{Cl} and ρ_{Cl} values for KCl crystals were taken from ref.[6].

5. The existence of high temperature non central motion was out of our consideration.

One can see from Fig. 3 that the energy potential in Rb_2SO_4 , Cs_2SO_4 crystals has two minima in (ab) plane with various depths. The big values of

E_a and E_0 parameters can be explained by assumed simplifications. The values of E_a and E_0 can decrease if one will take account the high temperature non central motion of thallium ions.

In order to define the changes in thallium local environment it is necessary to know the change of crystal field gradient. The gradient variation can changes the \hat{g} - and \hat{A} -tensor axes directions. In the assumption, that the axes of \hat{g} and \hat{A} tensor coincide [7], from the angular dependence of line positions for one of hyperfine transitions one can get the axes directions of \hat{g}^* -tensor with effective spin $S^*=1/2$. The angular dependence of line position is shown in Fig. 4. At temperatures higher than T^* the point symmetry of Tl^{2+} (II) center is C_1 . With cooling, below T^* the new thallium centers appears. One of the Tl^{2+} (II) centers (*a*) have higher line intensity than the other (*b* center). However the point symmetry of both centers remains unchanged. Main values and axes directions of effective \hat{g}^{2*} -tensors are different for Rb_2SO_4 , Cs_2SO_4 crystals. The projection of z -axis \hat{g}^{2*} -tensors of (*ab*) plane are shown in Fig. 3. One can see that z -axis projection direction corresponds to direction of maximal gradient of crystals field.

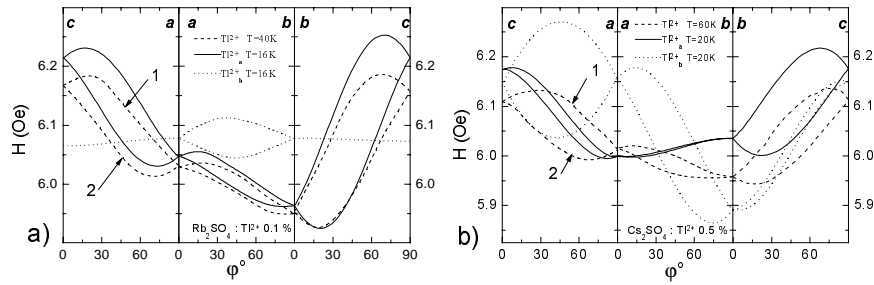


Figure 4: The angular dependence of EPR spectrum line positions for low-field hyperfine transitions of Tl^{2+} (II) ions in a) Rb_2SO_4 and b) Cs_2SO_4 crystals.

At $T > T^*$ the anomaly of the EPR linewidth angular dependence of Tl^{2+} (II) was observed (Fig. 5). In the case of averaging motion, EPR linewidth can be written as [4]

$$\delta H = \frac{(H_a - H_b)^2}{8AP_{act}} + \delta H_0, \quad (4)$$

where δH_0 - homogeneous linewidth (≈ 2 Oe.), H_a and H_b magnetic fields, which corresponds to the EPR line position of centers *a* and *b*. Neglecting the temperature dependence of spin hamiltonian parameters, one can define H_a and H_b from the angular dependence of line positions at $T < T^*$ (Fig. 4). We can calculate the angular dependence of EPR linewidth (Fig. 5 solid line). One can see that the simple model describes the change of EPR linewidth fairly well.

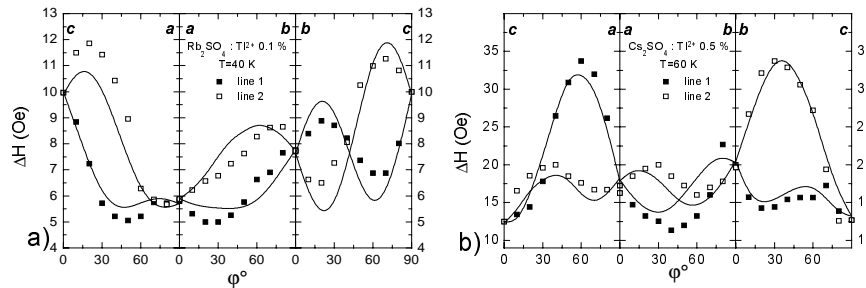


Figure 5: The angular dependence of EPR linewidth of $\text{Tl}^{2+}(\text{II})$ ions in a) Rb_2SO_4 and b) Cs_2SO_4 crystals.

So the low temperature anomaly of $\text{Tl}^{2+}(\text{II})$ ions EPR spectrum in Rb_2SO_4 , Cs_2SO_4 crystals can be explained by motion of $\text{Tl}^{2+}(\text{II})$ paramagnetic centers between two structural nonequivalent states arising near noncentral positions. These two structural nonequivalent states can be due to $\text{Tl}^{2+}(\text{II})$ ions displacements under the influence of electrostatic force.

The work was in part supported by the Russian State Foundation for Basic Research, Grant No 98-02-18037.

References

- [1] Efimov V.N., Mamin G.V. *Mod. Phys. Lett. B* **11**, 579 (1997)
- [2] Mamin G.V., Efimov V.N. *Mod. Phys. Lett. B* **12**, 929 (1998)
- [3] Abdulsabirov R.Ju., Stepanov V.G., Gresnev Ju.S., Zaripov M.A. *Fizika Tverdogo Tela* **14** 1816 (1972) (in Russian)
- [4] Carrington A., McLachlan A.D. *Introduction to magnetic resonance with application to chemistry and chemical physics*. Harper and Row publisher, 1967
- [5] Bokij G.B. *Kristallohimija*. Moscow, Nauka, 1978 (in Russian)
- [6] Kittel C. *Introduction to solid state physics*. Fourth edition, John Wiley & Sons, Inc., NY, 1976
- [7] Eremin M.V., Silkin N.I. *Phys. Stat. Sol.(b)* **84**, 803 (1977)